

Four-, Five- and Six-Coordinated Zn^{II} Complexes of OH-Containing Ligands: Syntheses, Structure and Reactivity

Mishtu Dey,^[a] Chebrolu Pulla Rao,^{*[a]} Pauli Saarenketo,^[b] Kari Rissanen,^[b] and Erkki Kolehmainen^[b]

Keywords: N,O ligands / X-ray diffraction / Hydrogen bonds / Metalloenzymes / Zinc

Four-, five- and six-coordinated complexes of Zn^{II} with OH-rich molecules possessing an ONO binding core were synthesized, characterized and their structures were established by single-crystal X-ray diffraction. The corresponding metal ion geometries were found to be distorted tetrahedral, square pyramidal and octahedral, respectively. The complexes exhibit interesting lattice structures such as layered and corrug-

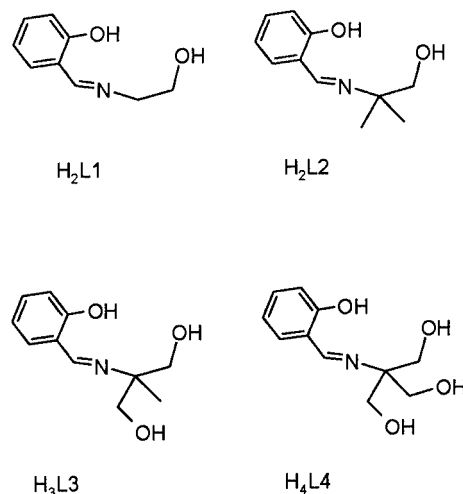
ated sheets owing to the presence of a number of weak intermolecular interactions. The five-coordinated, water-bound Zn^{II} complex was studied because of its putative hydrolysis property towards *p*-nitrophenyl acetate.

(© Wiley-VCH Verlag GmbH, 69451 Weinheim, Germany, 2002)

Introduction

Zinc is an essential element for all forms of life and is present at the active site of various enzymes.^[1] Zn^{II} is known to exhibit both catalytic and structural roles in its proteins and enzymes.^[2–4] The diversity in the functions of Zn^{II} is attributed to its versatile coordination chemistry. Hence, coordination compounds of Zn^{II} are used as biomimetic models.^[5–8] It is therefore important to understand how the Zn^{II} center controls the function of metalloenzymes.^[9] It may be noted that generally the geometry around the catalytic zinc is distorted and the coordination number varies between four, five and at times even six, along with the presence of labile ligands including a water molecule.^[2] While the biological functions of zinc in metalloproteins vary considerably, the active sites exhibit some common structural features.^[1] In several zinc enzymes, the metal center is coordinated through the N of histidine and O of aspartic or glutamic acid.^[10–12] The role of Zn^{II} in the active centers of hydrolytic metalloenzymes, such as carbonic anhydrase, carboxypeptidase and phosphatase, has constantly been a subject of interest in bioinorganic chemistry.^[13–15] Therefore we have chosen a series of hydroxy-rich molecules possessing tridentate ONO donor sites to study their coordination chemistry with Zn^{II}. The coordination behavior of OH-rich molecules has been demonstrated by us in the case of *cis*-VO₂⁺, *cis*-MoO₂²⁺ and *trans*-

UO₂²⁺ and Ti^{IV}, and by others in the case of iron and manganese, as reported recently in the literature.^[16–20] The present paper deals with the results of syntheses, characterization and crystal structure determinations of four-, five-, and six-coordinated Zn^{II} complexes of molecules possessing an ONO core. The ligands used in the study are shown in Scheme 1. A five-coordinated Zn^{II}–OH₂ complex was studied for its hydrolytic activity towards *p*-nitrophenyl acetate.



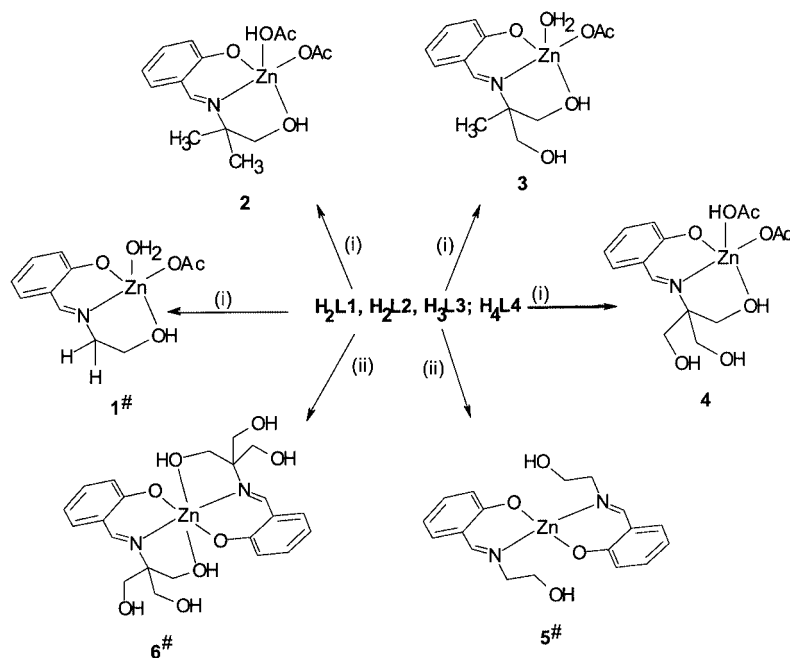
Scheme 1. Schematic representation of the ligands used

Results and Discussions

The reactions of Zn^{II} yielded complexes possessing one or two ligand moieties in its coordination sphere depending

^[a] Bioinorganic Laboratory, Department of Chemistry, Indian Institute of Technology Bombay, Mumbai 400 076, India
Fax: (internat.) +91-22/572-3480
E-mail: cpao@chem.iitb.ac.in

^[b] Department of Chemistry, University of Jyväskylä, Jyväskylä, 40351, Finland



Scheme 2. Zn^{II} complexes of OH-rich molecules; # structure was established by a single crystal XRD study; reaction conditions: (i) Zn(OAc)₂·2H₂O; Zn/L (1:1), CH₃OH; (ii) Zn(OAc)₂·2H₂O; Zn/L (1:2), CH₃OH

upon the ratio of metal to ligand (H₂L1 – H₄L4) used (1:1 or 1:2) as shown in Scheme 2. However, H₂L2 and H₃L3 resulted in the formation of the same type of complex, possessing only one ligand per metal ion whether the reaction was carried out in a 1:1 or 1:2 ratio. All the products exhibited similar types of coordination features among the 1:1 reactions no matter how many -OH groups were present in the ligands, H₂L1 (one), H₂L2 (one), H₃L3 (two) and H₄L4 (three). The complexes were all characterized by FTIR, UV/Vis, ¹H and ¹³C NMR spectroscopy, FAB mass spectrometry, and the structures of **1**, **5** and **6** were also established by single crystal XRD. The crystallographic data is given in Table 1. Further studies were performed on **1** to determine its effect on the hydrolysis of *p*NPA.

IR and UV/Vis Spectra

The IR spectra of the compounds **1–6** show ν_{OH} and $\nu_{\text{C=N}}$ vibrations at 3321–3390 and 1624–1638 cm⁻¹, respectively and the binding of the imine nitrogen was revealed by the lowering of the frequency (13–15 cm⁻¹). The ν_{asym} and ν_{sym} vibrations of the acetate group were observed in the regions, 1550–1570 and 1407–1445 cm⁻¹, respectively, with $\Delta\nu$ being 105–120 cm⁻¹, suggesting a monodentate binding of the acetate group.^[21] These were further confirmed from the single crystal XRD structure of **1**. An intense absorption band around 360 nm, due to the phenolate π - π^* transition, was observed in all cases. The π - π^* transition associated with the azomethine moiety showed a 10 nm blue shift in the complexes.

¹H NMR Spectroscopic Studies

The phenolic-OH proton signal disappeared from the spectra of all the complexes **1–6** due to the binding of this

moiety as Ph-O⁻ to Zn^{II}. The spectra also indicated a downfield shift in the azomethine (-CH=N) proton signal by about 0.2–0.3 ppm, suggesting the binding of this nitrogen to Zn^{II}. Complexes **1–4** and **6** exhibited one bound -CH₂OH (δ = 5.2–6.0 ppm, $\Delta\delta$ = 0.5 to 1.3 ppm), **2**, **4** and **6** exhibited one bound -CH₂OH and one or two free -CH₂OH groups (δ = 4.7–5.1 ppm, $\Delta\delta$ = 0.02 to 0.3 ppm), and **5** exhibited one free -CH₂OH (δ = 5.1 ppm). The signal at δ = 1.82 ppm indicates the presence of an acetate moiety in **1–4**. Thus, based on ¹H NMR spectra, it was possible to derive the primary coordination about Zn^{II}.

¹³C NMR Spectroscopic Studies

In **1–6** the azomethine (HC=N) carbon shifts downfield ($\Delta\delta$ = 6–14 ppm) relative to the corresponding ligand. Downfield shifts were also observed with the tertiary carbon ($\Delta\delta$ = 3–7 ppm) and with the bound -CH₂OH signals ($\Delta\delta$ = 0.7–4.2 ppm). In **1–4**, the presence of an acetate moiety was identified.

Mass Spectral Studies

The FAB mass spectra of all the complexes showed molecular ion peaks corresponding to their molecular weights as mentioned in the Exp. Sect.. The peak pattern and the intensity ratio confirms the isotopic ratio of M/M + 2/M + 4 peaks as 2.6:1.5:1.

Molecular and Crystal Lattice Structure of **1**

Complex **1** is neutral, five-coordinate and has the molecular formula [Zn(HL1)(OAc)(H₂O)], where HL1 acts as a tridentate ligand bound through O_{phen}, O_{alk} and N_{imi} groups. The fourth and fifth coordination sites are occupied

Table 1. Summary of crystallographic data for the complexes **1**, **5** and **6**

	1	5	6
Empirical formula	C ₁₁ H ₁₅ NO ₅ Zn	C ₁₈ H ₂₀ N ₂ O ₄ Zn	C ₂₃ H ₃₂ N ₂ O ₉ Zn
Molecular mass	306.61	393.73	545.88
<i>T</i> /K	173(2)	173(2)	123(2)
Crystal system	Orthorhombic	Monoclinic	Orthorhombic
Space group	<i>Pbca</i> (No. 61)	<i>Cc</i> (No. 9)	<i>Pbca</i>
<i>a</i> (Å)	10.797(1)	9.777(2)	11.166(10)
<i>b</i> (Å)	12.484(1)	10.522(2)	18.735(2)
<i>c</i> (Å)	17.997(1)	16.454(3)	22.496(2)
β (°)		90.66(2)	
<i>V</i> (Å ³)	2425.8(3)	1692.6(6)	4705.8(8)
<i>Z</i>	8	4	8
Absorption coefficient (m)/mm ⁻¹	2.037	2.241	1.101
<i>D</i> _{calcd.} (gcm ⁻³)	1.679	1.545	1.541
Total reflections	8785	1826	49183
Unique reflections	2762	1826	4142
Parameters	223	306	337
Final <i>R</i> [<i>I</i> > 2σ(<i>I</i>)]	0.0339	0.0270	0.0281
<i>R</i> _w ^[a]	0.0732	0.0692	0.0673

[a] Weighting scheme is as follows: **1**: calcd. $w = 1/[s^2(F_o^2) + (0.0172P)^2 + 1.4009P]$, where $P = (F_o^2 + 2F_c^2)/3$. **5**: calcd. $w = 1/[s^2(F_o^2) + (0.0583P)^2 + 0.8186P]$, where $P = (F_o^2 + 2F_c^2)/3$. **6**: calcd. $w = 1/[s^2(F_o^2) + (0.0275P)^2 + 5.0231P]$, where $P = (F_o^2 + 2F_c^2)/3$.

by an acetate group and a water molecule (Figure 1). The Zn–O_{phe}, Zn–O_{water}, Zn–N_{imi}, Zn–O_{acetate} and C–O_{acetate} distances were found to be consistent with those reported in the literature.^[21–24] In **1**, the trans angle [167.5(1)°], the angles in the basal plane [98.0(1) – 143.7(1)°] and the apical to basal angles [76.3(1) – 100.9(1)°], all indicate a distorted square-pyramidal geometry around the Zn^{II} center (Table 2). A Zn–O_{alk} distance of 2.419 Å observed for Zn–OHCH₂-binding in **1** is rather long when compared to that generally found in the literature for similar coordination. It is attributable to a weak binding as well as an increase in the coordination number from four to five. It has been noticed from O,N-bound Zn^{II} complexes in the literature that the common coordination number is four and when this number increases the additional coordinations are found to be generally weak with Zn^{II}...O distances ranging from 2.34 to 2.91 Å; the corresponding geometries are highly distorted.^[25–29] Such observations include a Zn^{II}...O_{phosphato} distance of 2.71 Å observed in the case of the Zn^{II}-ATP complex^[25] (distorted octahedral), Zn^{II}...O_{carboxylato} distances of 2.91 Å and 2.79 Å observed in the case of two Zn^{II}-histidino complexes,^[26,27] (distorted octahedral), Zn^{II}...O_{perchlorato} distances of 2.528 and 2.818 Å observed with the two crystallographically independent molecules present in the lattice of a Zn^{II}-triazacyclododecane complex^[28] (distorted trigonal bipyramidal), Zn^{II}...O_{crowner} distances of 2.34, 2.56 and 2.60 Å observed in the case of the Zn-crown ether complex^[29] (highly distorted trigonal bipyramidal).

Each molecule in the lattice of **1** interacts with three other neighbor molecules via two hydrogen bonds, resulting in a total of six hydrogen bonds. The phenoxy oxygen accepts a hydrogen bond from the -CH₂OH of a neighboring molecule. The Zn^{II}-bound water molecule exhibits two H-

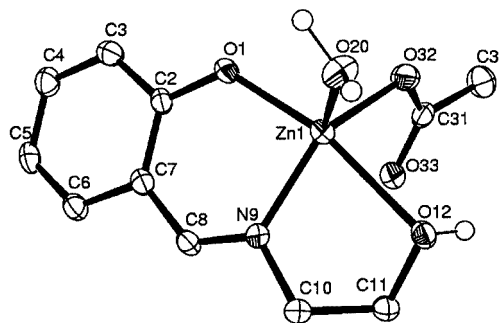


Figure 1. Molecular structure of **1** showing 50% probability thermal ellipsoids (ORTEP)

bond interactions as donors towards two different neighboring molecules. These H-bonds are accepted by the unbound oxygen of the acetate in the one case and the -CH₂OH group in the other case. Thus, both H₂O and -CH₂OH groups are involved in two H-bonds each (Figure 2). The packing of the molecules in the lattice is reminiscent of a layer type structure where the molecules are arranged to result in columns.

Molecular and Crystal Lattice Structure of **5**

Molecule **5** is neutral, having a molecular formula [Zn(HL1)₂] where each ligand is bidentately bound through O_{phen} and N_{imi} groups, thereby resulting in a distorted tetrahedral geometry around Zn^{II} (Table 2, Figure 3). In this structure, the -CH₂OH groups are not bound to the Zn^{II} center, with Zn...OH-CH₂ distances being 3.735 and 4.084 Å. In the crystal lattice of **5**, each Zn^{II} complex is involved in four intermolecular hydrogen bonds with four different

Table 2. Selected bond lengths (Å) and bond angles (deg)

1	5	6
Zn(1)–O(32) 1.960(2)	Zn(1)–O(1A) 1.923(2)	Zn(1)–O(1') 2.011(1)
Zn(1)–O(20) 2.006(2)	Zn(1)–O(1B) 1.929(2)	Zn(1)–O(1) 2.014(1)
Zn(1)–O(1) 2.025(2)	Zn(1)–N(9B) 2.001(2)	Zn(1)–N(7) 2.056(2)
Zn(1)–O(12) 2.419(2)	Zn(1)–N(9A) 1.984(2)	Zn(1)–N(7') 2.068(2)
Zn(1)–N(9) 2.017(2)		Zn(1)–O(11) 2.259(1)
		Zn(1)–O(11') 2.315(1)
O32–Zn1–O20 98.0(1)	O1A–Zn1–O1B 112.7(1)	O(1')–Zn(1)–O(1) 92.7(1)
O32–Zn1–N9 143.7(1)	O1A–Zn1–N9B 117.6(1)	O(1')–Zn(1)–N(7) 103.6(1)
O20–Zn1–N9 114.0(2)	O1B–Zn1–N9B 96.5(1)	O(1)–Zn(1)–N(7) 90.8(1)
O32–Zn1–O1 100.9(1)	O1A–Zn1–N9A 97.3(1)	O(1')–Zn(1)–N(7') 91.5(1)
O20–Zn1–O1 98.3(1)	O1B–Zn1–N9A 114.3(1)	O(1)–Zn(1)–N(7') 99.7(1)
N9–Zn1–O1 91.4(1)	N9B–Zn1–N9A 119.5(1)	N(7)–Zn(1)–N(7') 161.2(1)
O32–Zn1–O12 88.4(1)		O(1')–Zn(1)–O(11) 86.5(1)
O20–Zn1–O12 88.6(1)		O(1)–Zn(1)–O(11) 168.2(1)
N9–Zn1–O12 76.3(1)		N(7)–Zn(1)–O(11) 78.0(1)
O1–Zn1–O12 167.5(1)		N(7')–Zn(1)–O(11) 92.1(1)
		O(1')–Zn(1)–O(11') 164.8(1)
		O(1)–Zn(1)–O(11') 97.2(1)
		N(7)–Zn(1)–O(11') 87.9(1)
		N(7')–Zn(1)–O(11') 75.5(1)
		O(11)–Zn(1)–O(11') 86.2(1)

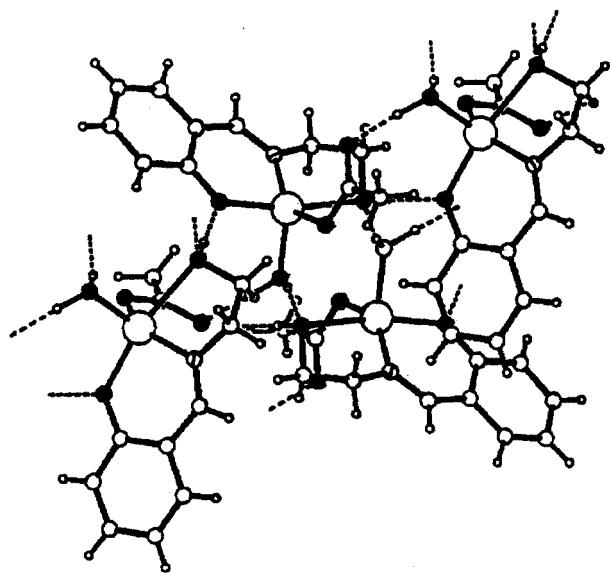


Figure 2. Lattice structure of **1** showing intermolecular hydrogen bond interaction (----); filled circles refer to oxygen, circles with a line refer to nitrogen and large circles refer to Zn^{II}

neighbors, of which two are of a donor type and the other two are of an acceptor type. While the O_{phe} acts as an acceptor, the $-CH_2OH$ group acts as a donor in these intermolecular interactions (Figure 4). The lattice structure of **5** shows a corrugated sheet pattern with the presence of channels as shown in Figure 5.

Molecular and Crystal Lattice Structure of **6**

Both the H_4L4 ligands act as monoanionic and tridentate binding through the O_{phen} , O_{alk} and N_{imi} groups to result in a distorted octahedral Zn^{II} complex, **6**, with the formula

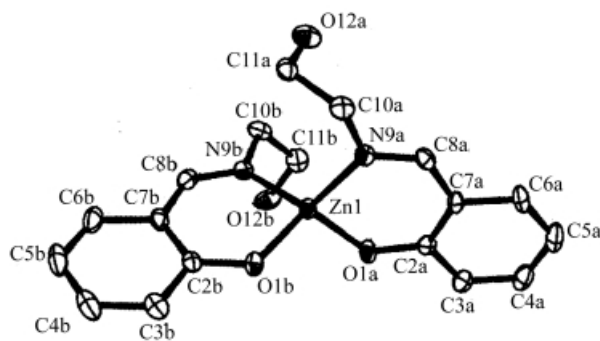


Figure 3. Molecular structure of **5** showing 50% probability thermal ellipsoids using ORTEP

$[Zn(H_3L4)_2]$ (Figure 6). Selected bond lengths and bond angles are shown in Table 2. Of the three $-CH_2OH$ groups, only one is bound to the zinc center ($Zn-O$ distances being 2.259 and 2.315 Å), whereas the other two remain free ($Zn-O$ distances being 4.25 to 5.41 Å); all these $-OH$ groups are involved in hydrogen-bonding interactions in the lattice. In the crystal lattice of **6**, all four of the oxygen atoms of each ligand are involved in hydrogen bond interactions. Compound **6** participates in intermolecular hydrogen bonds of the $O-H\cdots O$ type with five different neighbors in the lattice (Figure 7). While the O_{phe} acts as an acceptor, the $-CH_2OH$ groups act both as a donor and an acceptor. Both of the free CH_2OH groups exhibit two hydrogen bonds each whereas the bound CH_2OH group and O_{phe} exhibit only one hydrogen bond interaction. The lattice MeOH is involved in two H-bond interactions connecting two neighboring zinc complex units. Weak interactions present in all of these complexes exhibited a linear correlation between $d(D\cdots A)$ vs. $d(H\cdots A)$ as shown in Figure 8.

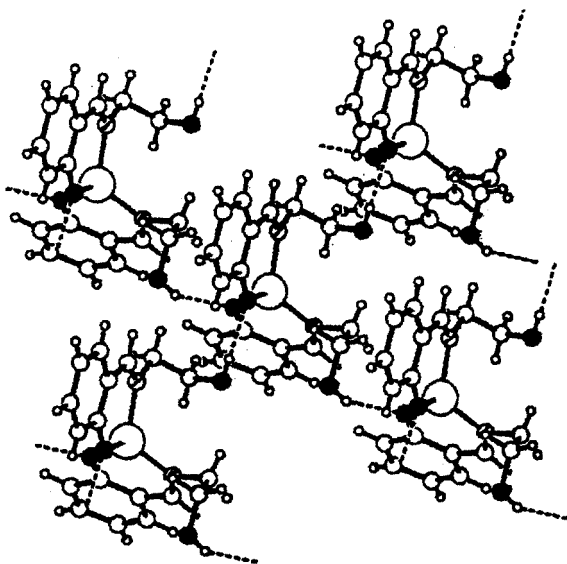


Figure 4. Lattice structure of **5** showing intermolecular hydrogen bond interactions (----); filled circles refer to oxygen, circles with a line refer to nitrogen and the large circles to the Zn^{II}

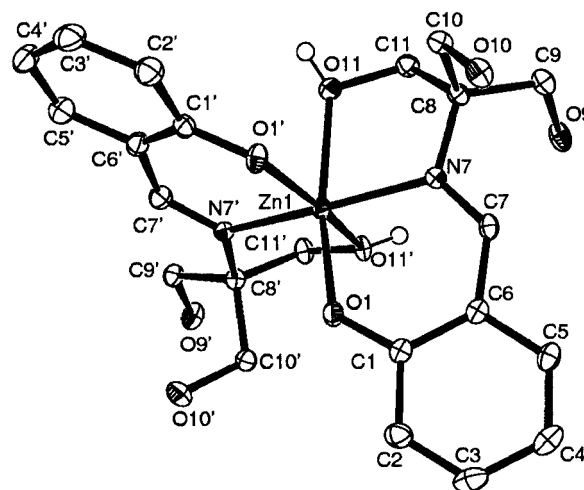


Figure 6. Molecular structure of **6** showing 50% probability of thermal ellipsoids using ORTEP

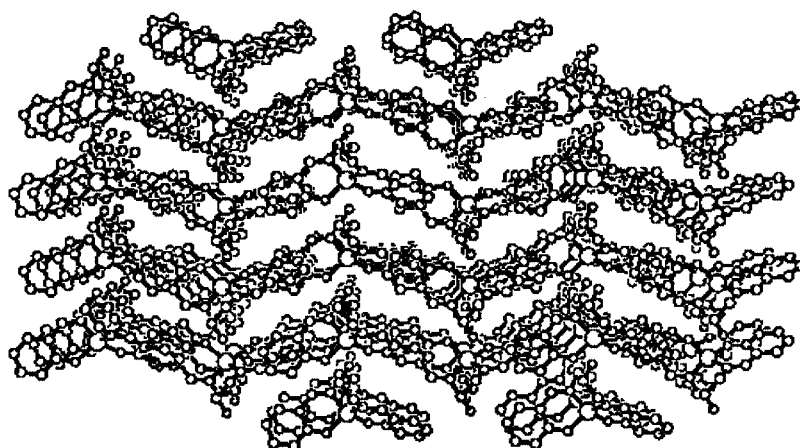


Figure 5. Lattice structure of **5** exhibiting corrugated sheet pattern

pH Titration

The potentiometric pH titration curves of H₂L1 in MeOH/water solution in the absence and in the presence of one equivalent of Zn(OAc)₂ are shown in Figure 9. A 0.1 M NaOH solution was used to titrate the Zn^{II}-coordinated water. The precursor ligand H₂L1 exhibited one sharp inflection with a pK_a of 9.14 corresponding to the phenolic moiety. On the other hand, the titration of H₂L1+Zn(OAc)₂ exhibited two inflection points. The first inflection observed at a pK_a of 6.93 corresponds to the deprotonation of the phenolic-OH followed by formation of a stable complex at pH > 6. This pK_a value for phenolate agrees well with that reported in the literature wherein deprotonation of the phenol was promoted by Zn^{II} coordination, with the pK_a shifting from 9.2 (without zinc) to 6.8 (with zinc).^[13] The second inflection point observed at pK_a 8.61 corresponds to the deprotonation of Zn^{II}-bound water

in the complex. This value was similar to the pK_a of 8.7 reported for bound H₂O in the case of a macrocyclic tetra-amine Zn^{II} complex,^[30] a model for carbonic anhydrase. A potentiometric pH titration experiment carried out under similar conditions with the isolated complex **1** also indicated an inflection point at a pK_a of 9.07, corresponding to the deprotonation of the Zn^{II}-bound aquo species.

Kinetics of the Hydrolysis of *p*-Nitrophenyl Acetate

The kinetics of *p*NPA hydrolysis in the presence and in the absence of zinc complex **1** was studied. The initial rate of the reaction was determined from the slope of a straight line obtained from the plot of the absorbance of *p*-nitrophenolate vs. time. The slope was calculated for the first 10% of the conversion from which the initial rate (*v*) of the

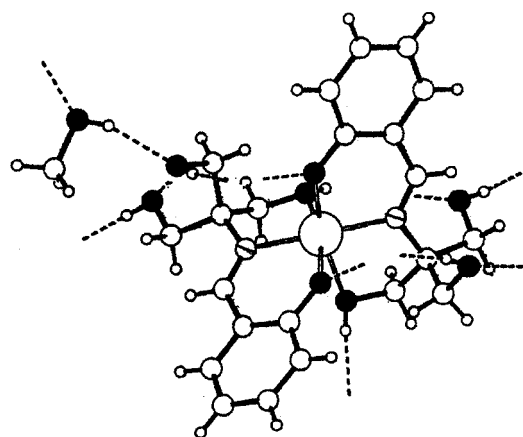


Figure 7. Structure of **6** showing intermolecular hydrogen bond interactions (---); filled circles refer to oxygen, circles with a line refer to nitrogen and the large circles to Zn^{II}

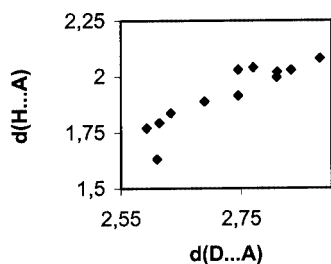


Figure 8. Plot of $d(\text{D}\cdots\text{A})$ vs. $d(\text{H}\cdots\text{A})$ using the hydrogen bond interaction data obtained in the lattices of **1**, **5** and **6**; $d(\text{D}\cdots\text{A})$ and $d(\text{H}\cdots\text{A})$ are in Å.

reaction was determined. Thus, these reactions yielded initial rates of 0.183×10^{-4} , 0.80×10^{-4} and $2.28 \times 10^{-4} \text{ ms}^{-1}$ at pH values of 7.2, 8.0 and 9.0, respectively, at 25 °C. The initial rate of hydrolysis increased when the pH of the reaction solution increased, owing to an increase in the concentration of the $\text{Zn}-\text{OH}^-$ species. The rate of hydrolysis was found to increase to $2.35 \times 10^{-4} \text{ ms}^{-1}$ at 35 °C and pH 8.0 as expected. The experimental results obtained at each stage were compared with the results of the corresponding control experiments.

Table 3. Hydrogen bond interaction data for **1**, **5** and **6**

D–H...A	$d(\text{H}\cdots\text{A})$	$d(\text{D}\cdots\text{A})$	$\angle\text{DHA}$	Symmetry
1				
O12–H12A...O1	1.837	2.633	176.9	$[x - 1/2, -y + 1/2, -z]$
O20–H20A...O33	1.631	2.610	169.0	$[x + 1/2, -y + 1/2, -z]$
O20–H20B...O12	2.030	2.745	168.7	$[-x, -y, -z]$
5				
O(12A)–H(12A)...O(1A)#1	2.02(6)	2.801(3)	164(5)	$[x + 1/2, y - 1/2, z]$
O(12B)–H(12B)...O(1B)#2	2.04(7)	2.770(3)	151(6)	$[x - 1/2, y - 1/2, z]$
6				
O(9)–H(9)...O(1')#1	1.770(17)	2.593(2)	170(3)	$x - 1/2, -y + 3/2, -z + 1$
O(10)–H(10)...O(9)#2	1.889(17)	2.689(2)	170(2)	$x + 1/2, -y + 3/2, -z + 1$
O(11)–H(11)...O(1M)	1.997(17)	2.809(2)	173(2)	
O(9')–H(9')...O(1)#3	1.793(17)	2.614(2)	171(2)	$x - 1/2, y, -z + 3/2$
O(10')–H(10')...O(9')#4	1.915(17)	2.745(2)	173(2)	$x + 1/2, y, -z + 3/2$
O(11')–H(11')...O(10)#1	2.028(17)	2.833(2)	172(2)	$x - 1/2, -y + 3/2, -z + 1$
O(1M)–H(1M)...O(10')#5	2.08(2)	2.881(2)	169(3)	$-x + 1, y + 1/2, -z + 3/2$

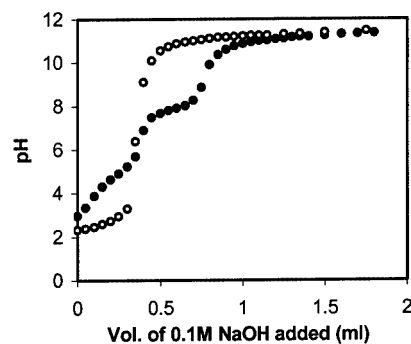
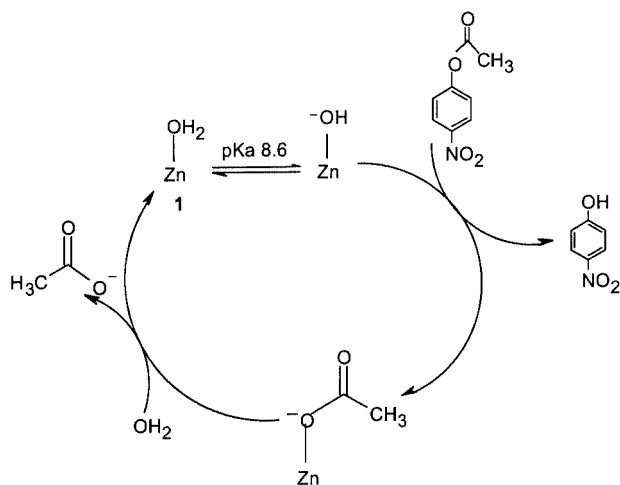


Figure 9. Experimental titration curves of $1.0 \times 10^{-3} \text{ M H}_2\text{L1}$ in the presence of $4.0 \times 10^{-3} \text{ M HCl}$ in aqueous methanol (33%, v/v) at 25 °C and $I = 0.1 \text{ M}$ (NaNO_3); (o) in the absence of Zn^{2+} and (•) in the presence of an equimolar amount of Zn^{2+}

Experiments were also carried out at a fixed concentration of **1** and variable concentrations of *p*NPA (*C*) and vice versa. The plot of $\ln v$ vs. $\ln C$ showed that the hydrolysis kinetics is first order with respect to the substrate as well as the zinc complex **1**, and second order overall. The second order rate constants (k_{obs}) were found to be 0.967×10^{-3} and $6.88 \times 10^{-3} \text{ M}^{-1}\text{s}^{-1}$ at pH 8.0 and 9.0, respectively. Based on the present studies it has been proposed that the water coordinated to the Zn^{II} center plays an important role in the hydrolysis process as indicated in Scheme 3. Four- or five-coordinated mononuclear Zn^{II} complexes of the type $\text{L}-\text{Zn}-\text{OH}_2$ have been used in the literature as model molecules for hydrolytic enzymes.^[31,32]

Conclusions

Complexes synthesized from the reaction of Zn^{II} with $-\text{OH}$ rich molecules exhibited varied structures and geometry. All these ligands are monoanionic and are bound to the zinc center, either in a bi- or tridentate fashion. This resulted in the formation of distorted geometries of tetrahedral (**5**), square pyramidal (**1**) and octahedral complexes (**6**). Thus, as we go from four- to five- to six-coordinated species, the coordination environment changes from N_2O_2



Scheme 3. Possible mechanism for *p*-nitrophenyl acetate hydrolysis by **1**

to NO₄ to N₂O₄ as derived from the crystal structures of **1**, **5** and **6**, respectively. The primary coordination spheres of these complexes are shown in Figure 10 for comparison. The number of chelate rings formed in these complexes increases from two (**5**) to three (**1**) to four (**6**) in the respective complexes. Interestingly, the five-coordinated zinc complex (HL1–Zn–OH₂) (**1**) exhibited an increased rate of hydrolysis of *p*NPA and hence is expected to possess a relationship with the Zn^{II} center, of relevance in zinc hydrolytic enzymes.

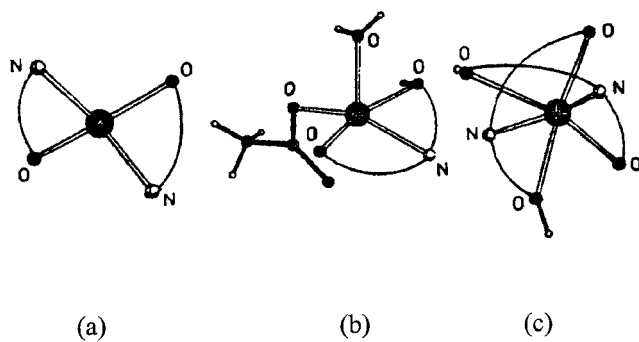


Figure 10. Structures representing primary coordination spheres of **1**, **5** and **6**; (a), (b) and (c) stand for **5**, **1** and **6**, respectively; big circles represent Zn

Experimental Section

General: Elemental analysis was carried out on a Carlo–Erba elemental analyzer. FTIR spectra were recorded on a Nicolet Impact 400 machine in a KBr matrix. UV/Vis spectrophotometric experiments were performed on a Shimadzu UV2101PC instrument equipped with a temperature controlled cell holder (TCC-260). ¹H and ¹³C NMR spectra were recorded on JEOL JNM GSX-270 FT or Varian XL-300 spectrometer in (CD₃)₂SO. The FAB mass spectra were recorded on a JEOL SX 102/DA-6000 Mass Spectrometer/Data System using Argon/Xenon (6 kV, 10 mA) as the carrier gas. The accelerating voltage was 10 kV and the spectra were recorded

at room temperature. *m*-Nitrobenzyl alcohol (NBA) was used as the matrix. All the chemicals used were procured from local sources and purified before use. All the solvents were purified and dried immediately before use. All complexes were isolated and purified by recrystallization before performing further studies.

Syntheses

H₂L1: 2-Amino-1-ethanol (1.05 g, 10 mmol) dissolved in MeOH (15 mL) was added to salicylaldehyde (1.0 mL, 10 mmol) in MeOH (15 mL). The reaction mixture was heated to 40 °C for 1 h and then cooled to room temperature followed by concentrating the resulting mixture to a liquid product. FTIR (KBr): $\tilde{\nu} = 3411$ (ν_{OH}), 1639 (ν_{C=N}) cm⁻¹. ¹H NMR ([D₆]DMSO): δ = 8.50 (s, 1 H, HC=N), 7.43 (d, 1 H, Ar H), 7.31 (t, 1 H, Ar H), 6.87 (m, 2 H, Ar H), 4.79 (s, 1 H, CH₂OH), 3.64 (s, 4 H, CH₂OH). The ligands **H₂L2**, **H₃L3** and **H₄L4** were synthesized adopting a similar procedure. The products were obtained as yellow solids by trituration with hexane and were further recrystallized from MeOH and then characterized.^[20]

[Zn(HL1)(CH₃COO)(H₂O)] (1**):** The reaction was carried out using a 1:1 mol ratio of the zinc acetate to the ligand. Zn(acetate)₂·2H₂O (0.2195 g, 1.0 mmol) in MeOH (10 mL) was added dropwise to H₂L1 (0.140 mL, 1 mmol) in MeOH (10 mL), and the resultant pale yellow reaction mixture was stirred at room temperature for an hour and then refluxed for 4 h. The reaction mixture was then cooled to room temperature and was concentrated to give a yellow mass, which was trituated with hexane resulting in an off-white product. The crude product was recrystallized from a methanol/hexane mixture (1:2 v/v) resulting in the formation of single crystals of **1** suitable for X-ray diffraction (XRD) studies. Yield: 0.269 g (88%); m.p. 128–132 °C. FTIR (KBr): $\tilde{\nu} = 3301$ (ν_{OH}), 1638 (ν_{C=N}) cm⁻¹. ¹H NMR ([D₆]DMSO): δ = 8.30 (s, 1 H, HC=N), 7.19 (d, 2 H, Ar H), 6.60 (d, 1 H, Ar H), 6.49 (t, 1 H, Ar H), 5.25 (br, 1 H, CH₂OH), 3.54 (m, 4 H, CH₂OH), 1.81 (s, 3 H, CH₃COO) ppm. ¹³C NMR: δ = 171.5 (HC=N), 176.8 (CH₃COO), 170.1, 135.8, 133.9, 122.2, 118.3, 113.1 (six Ar C), 61.4 (CH₂), 60.0 (CH₂OH), 22.6 (CH₃COO). C₁₁H₁₅NO₅Zn (306.6): calcd. C 43.09, H 4.93, N 4.57; found C 42.20, H 4.98, N 4.54%.

[Zn(H₃L4)(CH₃COO)(CH₃COOH)] (2**):** This compound was synthesized by adopting the procedure given for **1**, except that the ligand used was H₄L4. Yield: 0.445 g (77%); m.p. >200 °C. FTIR (KBr): $\tilde{\nu} = 3390$ (ν_{OH}), 1638 cm⁻¹ (ν_{C=N}). ¹H NMR ([D₆]DMSO): δ = 8.28 (s, 1 H, HC=N), 7.14 (m, 2 H, Ar H), 6.52 (d, 1 H, Ar H), 6.40 (t, 1 H, Ar H), 5.99 (br, 1 H, CH₂OH), 5.13 (br, 1 H, CH₂OH), 4.73 (br, 1 H, CH₂OH), 3.47 (s, 6 H, CH₂), 1.82 (s, 3 H, CH₃COO) ppm. ¹³C NMR: δ = 176.9 (HC=N), 170.3 (CH₃COO), 168.3, 136.3, 133.4, 122.3, 118.9, 112.3 (six Ar C), 65.4, (*tert* C), 64.6, (CH₂OH), 63.3, (CH₂OH), 23.1, (CH₂OH), 18.4, (CH₃COO). C₁₅H₂₁NO₈Zn (408.7): calcd. C 44.11, H 5.15, N 3.43; found C 44.40, H 4.90, N 3.50. FAB MS: *m/z* = 409 (10) [M⁺].

[Zn(HL2)(CH₃COO)(H₂O)] (3**):** Compound **3** was synthesized by adopting the procedure given for **1** but using H₂L2. Yield: 0.240 g (72%); m.p. >200 °C. FTIR (KBr): $\tilde{\nu} = 3231$, (ν_{OH}), 1634 cm⁻¹ (ν_{C=N}). ¹H NMR ([D₆]DMSO): δ = 8.38 (s, 1 H, HC=N), 7.21 (d, 1 H, Ar H), 7.12 (t, 1 H, Ar H), 6.56 (d, 1 H, Ar H), 6.42 (t, 1 H, Ar H), 5.76 (s, 2 H, CH₂OH, CH₃OH), 3.42 (s, 2 H, CH₂OH), 1.82 (s, 3 H, CH₃COO), 1.20 (s, 6 H, CH₃), 1.09 (s, 3 H, CH₃) ppm. ¹³C NMR: δ = 170.2 (HC=N), 177.9 (CH₃COO), 167.0, 136.3, 133.9, 122.5, 119.3, 113.4 (six Ar C), 68.1 (*tert* C), 60.8 (CH₂OH), 53.4 (CH₃OH), 24.9 (CH₃COO), 24.0, 23.6 (CH₃) ppm. C₁₃H₁₉NO₅Zn (334.7): calcd. C 46.66, H 5.72, N 4.19; found C 46.41, H 5.86, N 4.17. FAB MS: *m/z* = 334 (50) [M⁺].

[Zn(H₂L3)(CH₃COO)(CH₃COOH)] (4): Compound **4** was synthesized by adopting the procedure given for **1** with the use of H₃L3. Yield: 0.354 g (65%); m.p. >200 °C. FTIR (KBr): $\tilde{\nu}$ = 3388 (ν_{OH}), 1637 cm^{-1} ($\nu_{\text{C=N}}$). ¹H NMR ([D₆]DMSO): δ = 8.29 (s, 1 H, HC=N), 7.16 (m, 2 H, Ar H), 6.57 (d, 1 H, Ar H), 6.46 (t, 1 H, Ar H), 5.40 (br, 1 H, CH₂OH), 4.82 (br, 1 H, CH₂OH), 3.43 (d, 4 H, CH₂OH), 1.82 (s, 3 H, CH₃COO), 1.16 (s, 3 H, CH₃) ppm. ¹³C NMR: δ = 177.0 (HC=N), 170.3, (CH₃COO), 167.9, 136.2, 132.7, 122.3, 118.8, 112.5 (six Ar C), 65.4, (*tert* C), 64.6, (CH₂OH), 63.4 (CH₂OH), 23.2 (CH₃COO), 17.9 (CH₃). C₁₅H₂₁NO₇Zn (392.6): calcd. C 45.89, H 5.39, N 3.57; found C 46.29, H 5.42, N 4.00. FAB MS: m/z = 392 (20) [M⁺].

[Zn(HL1)₂] (5): This reaction was carried out using a 1:2 mol ratio of zinc acetate to ligand. Zn(acetate)₂·2H₂O (0.5 mmol, 0.110 g) in MeOH (25 mL) was added to H₂L1 (1 mmol, 0.140 mL) in MeOH (10 mL), and the resultant golden-yellow solution was refluxed for 4 h and then cooled to room temperature. The solvent was removed under vacuum and the resultant yellow residue was redissolved in MeOH (3 mL) and kept at room temperature, whereupon **5** separated out. Single crystals of **5** suitable for X-ray diffraction studies were grown from the methanolic solution of the product. Yield: 0.357 g (91%); m.p. 210–212 °C. FTIR (KBr): $\tilde{\nu}$ = 3328 (ν_{OH}), 1624 cm^{-1} ($\nu_{\text{C=N}}$). ¹H NMR ([D₆]DMSO): δ = 8.38 (s, 1 H, HC=N), 7.23 (m, 2 H, Ar H), 6.62 (m, 1 H, Ar H), 6.53 (m, 1 H, Ar H), 5.05 (s, 1 H, CH₂OH), 3.59 (m, 4 H, CH₂OH) ppm. ¹³C NMR: δ = 172.0 (HC=N), 170.1, 135.9, 134.1, 122.2, 118.3, 113.4 (Ar C), 61.9 (CH₂OH), 59.9 (CH₂) ppm. C₁₈H₂₀N₂O₄Zn (393.7): calcd. C 54.91, H 5.12, N 7.12; found C 55.40, H 5.21, N 6.74. FAB MS: m/z = 393 (70) [M⁺].

[Zn(H₃L4)₂] (6): A similar procedure was adopted for synthesizing compound **6** using the ligand H₄L4. Crystallization of the crude product from methanol resulted in single crystals of **6** suitable for XRD studies. Yield: 0.333 g (65%); m.p. >200 °C. FTIR (KBr): $\tilde{\nu}$ = 3333 (ν_{OH}), 1625 cm^{-1} ($\nu_{\text{C=N}}$). ¹H NMR ([D₆]DMSO): δ = 8.35 (s, 1 H, HC=N), 7.10 (m, 1 H, Ar H), 6.77 (d, 1 H, Ar H), 6.41 (d, 2 H, Ar H), 5.16 (br, 1 H, CH₂OH), 4.74 (br, 1 H, CH₂OH), 4.11 (br, 1 H, CH₂OH), 3.62 (s, 6 H, CH₂) ppm. ¹³C NMR: δ = 170.1 (HC=N), 168.9, 136.2, 132.1, 122.3, 118.5, 112.0 (Ar C), 67.1 (CH₂OH), 61.5 (CH₂OH), 61.4 (CH₂OH), 48.6 (*tert*-C) ppm. C₂₂H₂₈N₂O₈Zn (513.9): calcd. C 51.43, H 5.49, N 5.45; found C 51.16, H 6.07, N 4.73. FAB MS: m/z = 513 (95) [M⁺].

However, when 1:2 reactions were carried out using ligands H₂L2 and H₃L3 the products obtained were similar to the products of the 1:1 reaction (**3** and **4**).

Potentiometric pH Titration

Titrations were carried out at 25 ± 0.2 °C by means of a Control Dynamics pH meter with a combined glass electrode. The electrode was calibrated using standard aqueous buffers immediately before use. Solutions were made of aqueous methanol (33%, v/v) and the ionic strength was adjusted to 0.1 M using NaNO₃. A solution of H₂L1 (1.00 mM) with four equivalents of HCl (4.00 mM) in the absence and in the presence of one equivalent of zinc(II) ion was titrated with 0.1 M NaOH aqueous solution. For the titration, every increment of NaOH (50 μ L) was added with an equilibration time of 60 s after each addition.

Hydrolysis of *p*-Nitrophenyl Acetate (*p*NPA): The hydrolysis rate of *p*NPA in the presence of [Zn(HL1)(acetate)(H₂O)] (**1**) was measured by an initial-slope method following the absorbance increase in the 400 nm band of the released *p*-nitrophenolate species at 25 °C. Such experiments were carried out at a solution pH of 7.2, 8.0

and 9.0 and these were maintained using tris(hydroxymethyl)aminomethane (20 mM) with an ionic strength of 0.1 mM KNO₃. To increase the solubility of *p*NPA, 10% CH₃CN/H₂O solution was used. In a typical experiment, *p*NPA (c = 0.02–0.5 mM) and the complex, [Zn(HL¹)(acetate)(H₂O)] (c = 0.01–0.1 mM) in 10% CH₃CN/H₂O solution, were mixed at the appropriate pH (the control experiment does not contain the Zn^{II} complex) and the UV/Vis absorption spectra were measured as a function of time until no substantial increase was observed in the absorbance of the 400 nm band. Hydrolysis of *p*NPA was also studied at 35 °C at pH 8.00. Initial slopes were determined from the plots of the measured absorbance at 400 nm versus time.

X-ray Crystallography: Diffraction data were collected for **1** and **6** on a Nonius Kappa CCD machine in the ϕ scan + ω scan mode (Mo- K_{α}) and data for **5** were collected on a MACH3 detector in the ψ scan mode (Cu- K_{α}). The structures were routinely solved using SHELXS 97/SIR92 and refined using the SHELXL 97 program packages.^[33,34] The diagrams were generated using the ORTEP 3 and PLUTON 98 programs.^[35] The data were corrected for empirical absorption. Full-matrix least-squares refinement with anisotropic thermal parameters for all non-hydrogen atoms was used. The hydrogen atoms were treated as riding atoms with fixed thermal parameters. Other details of data collection and structure refinement are provided in Table 1.

CCDC-183936 (**1**), -183937 (**5**) and -183938 (**6**) contain the supplementary crystallographic data for this paper. These data can be obtained free of charge at www.ccdc.cam.ac.uk/conts/retrieving.html [or from the Cambridge Crystallographic Data Centre, 12, Union Road, Cambridge CB2 1EZ, UK; Fax: (internat.) +44-1223/336-033; E-mail: deposit@ccdc.cam.ac.uk].

Acknowledgments

CPR acknowledges the financial support from the Department of Science and Technology, New Delhi and the Council of Scientific and Industrial Research (CSIR), New Delhi. MD acknowledges the SRF fellowship from CSIR. We thank RSIC, CDRI Lucknow for Mass Spectral measurements and Mr. Kuppinen for some experimental help. We thank all three of the referees for their constructive suggestions.

- [1] W. N. Lipscomb, N. Straeter, *Chem. Rev.* **1996**, *96*, 2375.
- [2] B. L. Vallee, D. S. Auld, *Biochemistry* **1990**, *29*, 5647; B. L. Vallee, D. S. Auld, *Biochemistry* **1993**, *32*, 6493.
- [3] *Hydrolytic Enzymes* (Eds.: A. Neuberger, K. Brocklehurst), Elsevier Science: Amsterdam, **1987**.
- [4] *Zinc Enzymes* (Eds.: I. Bertini, C. Luchinat, W. Maret, M. Zeppezauer), Birkhäuser: Boston, **1986**.
- [5] R. H. Prince, in *Comprehensive Coordination Chemistry* (Eds.: G. Wilkinson, R. D. Gillard, J. A. McCleverty), Pergamon Press: Oxford, U. K., **1987**, *5*, 925.
- [6] E. Kimura, T. Koike, *Chem. Commun.* **1998**, 1495, and references therein.
- [7] M. Ruf, K. Weis, H. Vahrenkamp, *J. Am. Chem. Soc.* **1996**, *118*, 9288.
- [8] A. Looney, G. Parkin, R. Alsasser, R. Ruff, H. Vahrenkamp, *Angew. Chem. Int. Ed. Engl.* **1992**, *31*, 92.
- [9] J. E. Coleman, *Zinc Enzymes*, Birkhauser, Boston, **1986**, 49.
- [10] D. C. Rees, M. Lewis, W. N. Lipscomb, *J. Mol. Biol.* **1983**, *168*, 367.
- [11] E. E. Kim, H. W. Wyckoff, *J. Mol. Biol.* **1991**, *218*, 449.
- [12] P. A. Frey, S. A. Whitt, J. B. Tobin, *Science* **1994**, *264*, 1927.
- [13] E. Kimura, *Acc. Chem. Res.* **2001**, *34*, 171.
- [14] H. Sigel, R. B. Martin, *Chem. Soc. Rev.* **1994**, *94*, 83.

- [15] J. P. Glusker, *Adv. Protein Chem.* **1991**, *42*, 1.
- [16] [16a] C. R. Cornman, G. J. Colpas, J. D. Hoeschele, J. Kampf, V. L. Pecoraro, *J. Am. Chem. Soc.* **1992**, *114*, 9925. [16b] C. J. Carrano, C. M. Nunn, R. Quan, J. A. Bonadies, V. L. Pecoraro, *Inorg. Chem.* **1990**, *29*, 944. [16c] X. Li, M. S. Lah, V. L. Pecoraro, *Inorg. Chem.* **1998**, *27*, 4567.
- [17] J. A. Bonadies, C. J. Carrano, *J. Am. Chem. Soc.* **1986**, *108*, 4088.
- [18] [18a] D. Rehder, C. Weidemann, A. Duch, W. Priebsch, *Inorg. Chem.* **1988**, *27*, 584. [18b] V. Vergopolous, W. Priebsch, M. Fritsch, D. Rehder, *Inorg. Chem.* **1993**, *32*, 1844.
- [19] [19a] D. C. Crans, R. A. Felty, O. P. Anderson, M. M. Miller, *Inorg. Chem.* **1993**, *32*, 247. [19b] D. C. Crans, R. W. Marshman, M. S. Gottlieb, O. P. Anderson, M. M. Miller, *Inorg. Chem.* **1992**, *31*, 4939. [19c] D. C. Crans, H. Chen, O. P. Anderson, M. M. Miller, *J. Am. Chem. Soc.* **1993**, *115*, 6769. [19d] D. C. Crans, P. M. Ehde, P. K. Shin, L. Pettersson, *J. Am. Chem. Soc.* **1991**, *113*, 3728. [19e] D. C. Crans, P. K. Shin, *J. Am. Chem. Soc.* **1994**, *116*, 1305. [19f] D. C. Crans, H. Chen, R. A. Felty, *J. Am. Chem. Soc.* **1992**, *114*, 4543.
- [20] [20a] G. Asgedom, A. Sreedhara, J. Kivikoski, J. Volkonen, E. Kolehmainen, C. P. Rao, *Inorg. Chem.* **1996**, *35*, 5674. [20b] G. Asgedom, A. Sreedhara, J. Kivikoski, J. Volkonen, C. P. Rao, *J. Chem. Soc., Dalton Trans.* **1995**, 2459. [20c] C. P. Rao, A. Sreedhara, P. V. Rao, B. M. Verghese, K. Rissanen, E. Kolehmainen, N. K. Lokanath, M. A. Sridhar, J. S. Prasad, *J. Chem. Soc., Dalton Trans.* **1998**, 2383 and refs. therein. [20d] P. V. Rao, C. P. Rao, E. K. Wegelius, K. Rissanen, E. Kolehmainen, *J. Chem. Soc., Dalton Trans.* **1999**, 4469. [20e] P. V. Rao, C. P. Rao, A. Sreedhara, E. K. Wegelius, K. Rissanen, E. Kolehmainen, *J. Chem. Soc., Dalton Trans.* **2000**, 1213.
- [21] G. B. Deacon, R. J. Phillips, *Coordn. Chem. Rev.* **1980**, *33*, 227.
- [22] C. O. Rodriguez, C. O. R. de Barbarin, N. A. Bailey, D. E. Fenton, Q.-Y. He, *J. Chem. Soc., Dalton Trans.* **1997**, 161.
- [23] A. Erxleben, J. Hermann, *J. Chem. Soc., Dalton Trans.* **2000**, 569.
- [24] A. Abufarag, H. Vahrenkamp, *Inorg. Chem.* **1995**, *34*, 2207.
- [25] P. Orioli, R. Cini, D. Donati, S. Mangani, *J. Am. Chem. Soc.* **1981**, *103*, 4446.
- [26] M. M. Harding, S. J. Cole, *Acta Crystallogr.* **1963**, *16*, 643.
- [27] R. H. Kretsinger, F. A. Cotton, R. F. Bryan, *Acta Crystallogr.* **1963**, *16*, 651.
- [28] S. C. Rawle, A. J. Clarke, P. Moore, N. W. Alcock, *J. Chem. Soc., Dalton Trans.* **1992**, 2755.
- [29] A. B. Charette, J.-F. Marcoux, F. Bélanger-Gariépy, *J. Am. Chem. Soc.* **1996**, *118*, 6792.
- [30] P. Woolley, *Nature* (London) **1975**, *258*, 677.
- [31] T. Koike, E. Kimura, *J. Am. Chem. Soc.* **1991**, *113*, 8935.
- [32] E. Kimura, I. Nakamura, T. Koike, M. Shionoya, Y. Kodama, T. Ikeda, M. Shiro, *J. Am. Chem. Soc.* **1994**, *116*, 4764.
- [33] *SHELX97 Programs for Crystal Structure Analysis (Release 97-2)*, G. M. Sheldrick, Institut für Anorganische Chemie der Universität, Tammanstrasse 4, 3400 Göttingen, Germany, **1998**.
- [34] SIR92 – A program for crystal structure solution: A. Altomare, G. Cascarano, C. Giacovazzo, A. Guagliardi, *J. Appl. Crystallogr.* **1993**, *26*, 343.
- [35] [35a] M. N. Burnett, C. K. Johnson, ORTEP III, Report ORNL-6895, Oak Ridge National Laboratory, Oak Ridge, TN, **1996**. [35b] A. L. Spek, *Acta Crystallogr., Sect. A* **1990**, *46*, C34.

Received December 19, 2001

[I01514]